ASSESSMENT OF CENTENNIAL (1918 – 2019) DROUGHT FEATURES IN THE CAMPANIA REGION BY HISTORICAL IN SITU MEASUREMENTS (SOUTHERN ITALY)

Antonia Longobardi[1], Ouafik Boulariah[1], Paolo Villani[1]

[1]Civil Engineering Department, University of Salerno, Fisciano, 84084, Italy

Correspondence to: Antonia Longobardi (alongobardi@unisa.it)

Abstract

Drought is a sustained period of below-normal water availability. It is a recurring and worldwide phenomenon, but the Mediterranean basin is seen as a very vulnerable environment in this perspective and understanding historical drought conditions in this area is necessary to plan mitigation strategies to further face future climate change impacts. The reported research was aimed at the description of drought conditions and evolution for the Campania region (Southern Italy), assessed by the analysis of an in-situ measurement database which covers a centennial period from 1918-2019. Standardized precipitation Index (SPI) time series were reconstructed for different accumulation time scales (from 3 to 48 months) and the Modified Man Kendall and Sen's test were applied to identify SPI changes over time. SPI time series were mostly affected by a negative trend, significant for a very large area of the region, particularly evident for the accumulation scales larger than 12 months. Mean drought duration (MDD), severity (MDS) and peak (MDP) were furthermore investigated for both moderate (SPI ≤ -1) and extremely severe conditions (SPI ≤ -2). The accumulation scale affected the drought features, with longer duration and larger severity associated to the larger accumulation scales. Drought characteristics spatial patterns were not congruent for the different SPI time scales: if duration and severity were larger in the southern areas, peaks appeared mostly severe in the northern areas of the region. Extremely severe events were featured by lower durations and larger severity compared to the moderate drought events but were very less frequent (over 75% less then) and did not appeared to be focused on specific areas of the region.

1 Introduction

Drought is a natural local or regional disaster which affects agricultural, hydrological, socio-economic, groundwater systems (Dracup et al., 1980;Mishra and Singh, 2010;Wilhite and Glantz, 1985). The climate change is likely to accelerate the climate-meteo-hydrological processes able to lead toward intense drought episodes in specific environments (Longobardi and Van Loon, 2018) and, in this perspective, in recent years and in several world regions, the drought evolution has been widely discussed and analyzed.

In different areas of Asia, the spatio-temporal variability of drought has been discussed by Zhang and Zhou (2015) and by Hasegawa et al. (2016). In America, regional drought events have been reviewed by Swain and Hayhoe (2015), Littell et al. (2016) and Sobral et al. (2019). Spinoni et al. (2015) and Stagge et al. (2017) analyzed drought events in different region of Europe. In particular for this specific geographical context, according to the IPCC fifth Assessment Report (AR5), the Mediterranean basin is seen as a very vulnerable environment (IPCC, 2014) and a number of regional scale drought analyses have been indeed performed in different regions of this area (Cook et al., 2016;Gouveia et al., 2017;Ruffault et al., 2018;Caloiero et al., 2019;Yves et al., 2020). At the global scale, south America, the Sahel, the Congo River Basin and the north-eastern China, besides the Mediterranean basin, resulted as the areas most frequently affected by severe droughts (Spinoni et al., 2019).

~~The Italian territory is vulnerable to drought episodes and the lack of observed reliable climate data by rain gauge station at the national level makes difficult temporal and spatial evaluation at a spatial resolution adequate to the interpretation of the effects associated to the precipitation scarcity. Additionally, data from global weather dataset could be used but their coarse spatial resolution makes them poorly effective because of the high precipitation variability that affects the southern Europe regions indeed. In this context, historical in-situ long term measurements are crucial for understanding historical drought conditions, in the way it is possible to learn about how a specific region would be affected by precipitation shortage periods, how severe would be the response and how quickly would it take to recover (Bonaccorso and Aronica, 2016; Marini et al., 2019). This information is important to set drought forecasting strategies which could help in preparedness actions, planning mitigation and adaptation strategies to projected climate changes (Peres et al., 2020; Gaitan et al., 2020)~~

The Italian territory is vulnerable to drought episodes and unfortunately the temporal consistency and the spatial resolution of available data by rain gauge stations is frequently inadequate for drought characterization analysis. Beyond ground rainfall observations, data from global weather datasets can be considered but their coarse spatial resolution makes them poorly effective especially in capturing the high precipitation variability that affects the southern Europe regions indeed. In this context, historical in-situ long term measurements are crucial for understanding historical drought conditions, as they allow to learn about how a specific region has been affected by precipitation shortage periods in the past, how severe was be the response and how quickly it took to recover from drought conditions (Bonaccorso and Aronica, 2016; Marini et al., 2019). This information is important to set drought forecasting strategies which could help in preparedness actions, planning mitigation and adaptation strategies to projected climate changes (Peres et al., 2020; Gaitan et al., 2020).

One of the widely used approach to define drought conditions and persistence consists in the use of mathematical indices, known as drought indicators, such as the Palmer Drought Severity Index (PDSI) (Palmer, 1965), the Crop Moisture Index (CMI) (Palmer, 1968), the Normalized Difference Vegetation Index (NDVI) (Rouse et al., 1974), the Standardised Precipitation Index (SPI) (McKee et al., 1993;Ganguli and Reddy, 2014), the Drought Recognition Index (RDI) (Tsakiris and Vangelis, 2005) and the Standardised Precipitation Evapotranspiration Index (SPEI) (Vicente-Serrano et al., 2010). In

particular the SPI, despite the inherent limitations, was considered in several studies to investigate drought characteristics across the world (Mishra and Singh, 2010;Van Loon, 2015).

For what concerns the Italian territory, Capra et al. (2012) investigated the spatio-temporal variability of drought at short and medium accumulation scale in the Calabria region, southern of Italy, using the SPI index, concluding that approximately half of the region was impacted by drought during the period 1981-1990, when the region suffered its worst drought. Di Lena et al. (2014) analysed drought periods in the Abruzzo region, showing a general downward trend in SPI time series, more pronounced on longer accumulation time scales. Marini et al. (2019) investigated droughts in Apulia region using the SPI and the RDI indexes, finding an upward trend in the severity of droughts in the western part and a downward trend in the eastern region. By applying the SPI index over 3 and 6-months for a short term and 12, 24-months for a long term, Caloiero et al. (2018) analysed dry and wet period in southern Italy, showing that when long-term precipitation scales are included, the probabilities of occurrence of dry conditions are higher than the wet one.

The reported case study is represented by the Campania region, located in southern Italy, a large area of about ~~14000~~ 13600 km^2, stretching from the Apennine Mountains to the Mediterranean Sea with a progressively decreasing elevations moving from the inlands to the coastline. The climate regime of the study area is typically seasonal with some evident differences depending on the location (Longobardi and Villani, 2010;Longobardi and Mautone, 2015;Longobardi et al., 2016; Longobardi and Boulariah, under review). Two distinct rain gauge networks are available for the region, one for the period 1918-1999 and the other for the period 2000-2019. They are characterized by different stations consistency, localisation and typology. With the aim to reconstruct continuous long-term monthly scale precipitation time series, the in-situ point measurements (observed at the rain gauge locations) for the two datasets were projected on a 10 x10 km resolution grid covering the whole region by using a geostatistical interpolation approach (Boulariah et al., 2020). Projecting the two distinct database point measurements to a common grid, made it possible the reconstruction of centennial historical time series of monthly precipitation time series from 1918-2019 crucial for long term historical drought conditions analysis.

The reconstructed gridded precipitation database was used to compute the Standardized Precipitation Index at different accumulation time steps, from SPI_3 to SPI_48, to explore the full range of drought definitions. SPI time series were analyzed for their spatial and temporal patterns features and the Modified Mann-Kendall and the Sen's slope test were used to assess the trend significance and magnitude. Additionally, the spatial patterns of drought characteristics were evaluated with the assessment of probability of occurrence, drought duration, drought severity and drought peak value, for different SPI thresholds, according to the run theory (Yevjevich, 1967).

The findings of the study in terms of detailed spatial and temporal characterization of drought conditions within the Campania region, represent an essential information for sustainable and efficient water resources management planning strategies.

2 Material and methods

2.1 Study area

The Campania region is located between 40.0 and 41.5° N and 13.5-16.0° E, covering about 13600 km^2 in the southwest of Italy (Figure 1).

The region is well known for a complex orography; the altitude of the region ranges from well above 2000 m a.s.l. in the Apennine Mountains to the coastline. The region is characterized by a complex climatic pattern, because of the orography. The seasonality is ~~quite marked~~well defined, with the larger amount of precipitation recorded during the winter periods. The mean annual rainfall of the study area ranges from 600 to 2400 mm whereas the average annual temperature is around 17ºC. Trend in historical precipitation and their seasonal variability were described in Longobardi and Villani (2010) and Longobardi et al. (2016). The area is experiencing a moderate negative trend in precipitation, especially for what concerns the north-east and south-west areas. At the same time, also the seasonal variability appeared to be featured by a negative trend, with a transition of the precipitation regime from a seasonal to more uniform one.

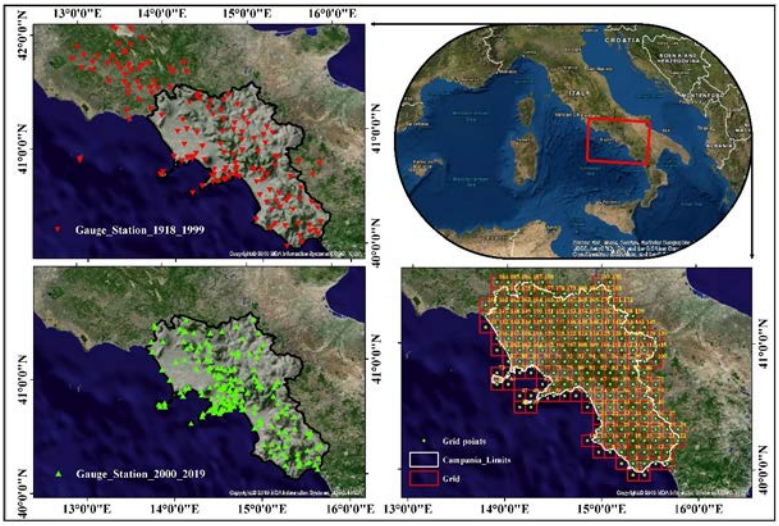

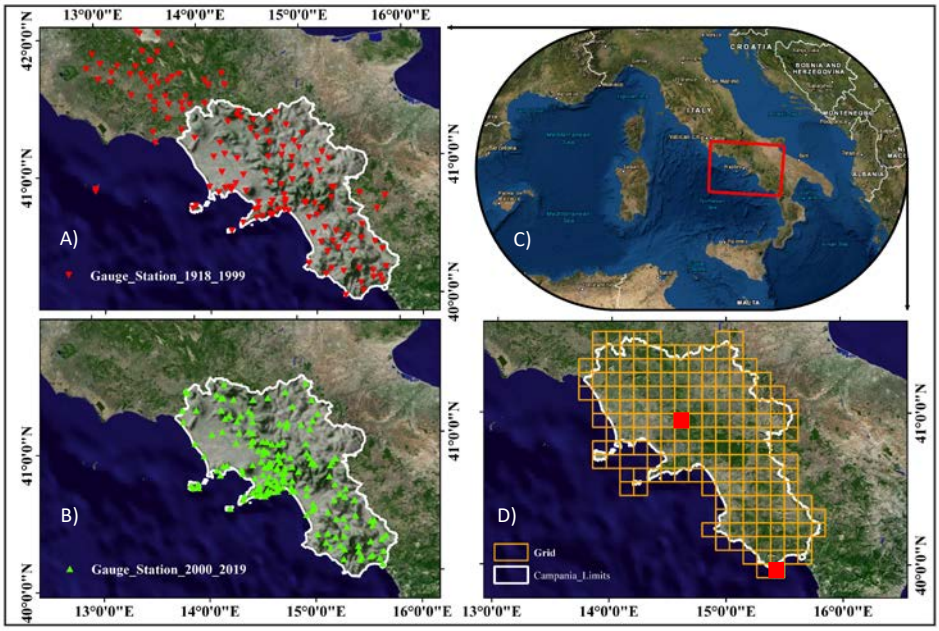

Figure 1: The studied area. ~~Left panel~~Panels A) and B): the two rain gauge networks. Panel C): the study area in the red box. Panel D): ~~Middle panel:~~ the grid shape for the region under investigation. Red boxes represent grid cells #2 and #108 reported in Figure 3. ~~Precipitation data are referred to the centre of each cell. Right panel: the region under investigation~~.

2.2 Dataset

As mentioned in the introduction, the gridded datasets used in the current paper was obtained from the research carried out by Boulariah et al. (2020), where different spatial interpolation approaches (both deterministic and geostatistical approaches), were applied to merge two monthly precipitation rain gauge (point) database available for the studied region, as they are different in rain gauge locations and moreover cover different periods of time, being one referred to the period 1918-1999 and the second to 2000-2019 (Figure 1 left panel). The number of a~~A~~vailable rain gauge stations were 154 and 187 respectively for the first period and the second period. Comparing the two considered periods of time, rain gauge density is then rather similar and rain gauge stations are similarly distributed over the region, with an exception for the Peninsula Sorrentina, a coastline area at the middle latitude of the region. The two-point dataset (rain gauges dataset) where spatially interpolated by the cokriging, which was found to be the best interpolating method over the investigated area based on the results of an

Tabella formattata

interpolation approaches comparative study, due to the high correlation (≥70%) between elevation and observed precipitation (Boulariah et al., 2020). The interpolated precipitation field (for each month and for each year) were projected on a high-resolution grid base (10 x 10 km). The result of the merging process was monthly gridded rainfall data from 1918 to 2019 for 191 high resolution grid points covering the whole of the Campania region, which were considered for the proposed analysis (Figure 1, middle panel).

Commentato [AL(1]: Notation 0.09°x0.09° was removed in the first round of the revision.

2.3 The Standardized Precipitation Index

The formulation of the SPI drought index for any given location is based on the cumulative rainfall record over a selected time scale and the probability density function "Gamma" which fit only positive and null values (McKee et al., 1993; Husak et al., 2007). In the literature and according to different previous studies, the rainfall time series are first fitted to the Gamma distribution and then standardized by transformation into a normal distribution (Caloiero et al., 2018;Martinez et al., 2019;Stagge et al., 2015;Zhou and Liu, 2016). The probability density function for the Gamma distribution can be expressed by the following equation:

$$g(x) = \frac{1}{\beta^{\alpha}\Gamma(\alpha)} x^{\alpha-1} e^{-x/\beta} \quad (1)$$

Where α, β and x are respectively the shape parameter, the scale parameter and the amount of precipitation (α, β and x > 0). Γ(α) is the gamma function expressed as:

$$\Gamma(\alpha) = \int_0^{\infty} y^{\alpha-1} e^{-y} \mathrm{d}y \quad (2)$$

Parameters $\hat{\alpha}$ and $\hat{\beta}$ are assessed through the maximum likelihood method (McKee et al., 1993;Liu et al., 2016):

$$\hat{\alpha} = \frac{1}{4A}\left(1+\sqrt{1+\frac{4A}{3}}\right) \text{ and } \hat{\beta} = \frac{\overline{x}}{\hat{\alpha}} \quad (3)$$

where

$$A = \ln(\overline{x}) - \frac{\sum \ln(x)}{n} \quad (4)$$

for n observations. By integrating the density of probability function g(x), the cumulative probability G(x) is obtained:

$$G(x) = \int_0^x g(x)dx = \frac{1}{\hat{\beta}\Gamma(\hat{\alpha})} = \int_0^x x^{\hat{\alpha}-1} e^{-\frac{x}{\hat{\beta}}} \mathrm{d}x \quad (5)$$

Given the Gamma distribution is not defined for x values equal to zero and that instead the cumulative rainfall series may contain null values, the cumulative distribution is re-defined as follows:

$$H(x)=q+(1-q)\,G(x) \quad (6)$$

where q is the probability of zero precipitation. Then, the value of the SPI can be obtained through the approximation proposed in Abramowitz and Stegun (1964) which converts the cumulative distribution H(x) to a normal random variable Z:

$$Z = \mathrm{SPI} = \begin{cases} -\left(t - \dfrac{c_0 + c_1 t + c_2 t^2}{1 + d_1 t + d_2 t^2 + d_3 t^3} \right), & \text{for } 0 < H(x) \le 0.5 \\ +\left(t - \dfrac{c_0 + c_1 t + c_2 t^2}{1 + d_1 t + d_2 t^2 + d_3 t^3} \right), & \text{for } 0.5 < H(x) \le 1 \end{cases} \quad (7)$$

$$t = \begin{cases} \sqrt{\ln\left[\dfrac{1}{(H(x))^2}\right]}, & \text{for } 0 < H(x) \le 0.5 \\ \sqrt{\ln\left[\dfrac{1}{(1-H(x))^2}\right]}, & \text{for } 0.5 < H(x) \le 1 \end{cases} \quad (8)$$

where:

$c_0 = 2.515517, c_1 = 0.802853, c_2 = 0.010328$

$d_0 = 1.432788, d_1 = 0.189269, d_2 = 0.001308$

SPI time series for different accumulation periods of 3, 6, 12, 24, 36 and 48 months (respectively SPI_3, SPI_6, SPI_12, SPI_24, SPI_36 and SPI_48) were computed for the studied dataset and used to describe wet and dry conditions according to the following values (McKee et al., 1993):

SPI Values	Drought severity
SPI ≥ 2.0	Extremely wet
1.5≤ SPI < 2.0	Very wet
1.0 ≤ SPI < 1.5	Moderately wet
-1.0 < SPI < 1.0	Near normal
-1.5 < SPI ≤ -1.0	Moderately dry
-2.0 < SPI ≤ -1.5	Severely dry
SPI < -2.0	Extremely dry

Table 1: classification of wet and dry conditions according to SPI values (Mc Kee et al., 1993).

2.4 Trend analysis

Time series of SPI were tested for trend detection in time. A trend is a significant change over time exhibited by a random variable, detectable by statistical parametric and non-parametric procedures. Provided the intrinsic autocorrelation of the analyzed time series, the current study provided results for non-parametric Modified Mann-Kendall (MMK) and Sen's test approaches. Those methods are briefly described in the following.

The Mann-Kendall test (Mann, 1945;Kendall, 1948) is one of the most widely used methods to detect trend in climatology analysis. It is used to analyze data collected over time for consistently increasing or decreasing trends (monotonic). It is a non-parametric test, which means it works for all distributions, thus tested data does not have to meet the assumption of normality but should have no serial correlation. The Mann-Kendall statistic S is defined as:

$$S = \sum_{i=1}^{n-1} \sum_{j=i+1}^{n} sign(x_j - x_i) \quad (9)$$

Codice campo modificato

where:

$$sign(x_j - x_i) = \begin{cases} +1, \text{ if } (x_j - x_i) > 1 \\ 0 \text{ , if } (x_j - x_i) = 0 \\ -1, \text{ if } (x_j - x_i) < 1 \end{cases} \quad (10)$$

Codice campo modificato

x_i and x_j are the annual values in years i and j, with i > j. When n ≥ 10, the statistic S is almost normally distributed with mean E(S) and variance Var(S) as follows:

$$E(S) = 0, \quad Var(S) = \frac{n(n-1)(2n+5)}{18} \quad (11)$$

however, the expression of Var(S) should be adjusted when tied value do exist:

$$Var(S) = \frac{1}{18}\left[n(n-1)(2n+5) - \sum_{p=1}^{q} t_p(t_p - 1)(2t_p + 5) \right] \quad (12)$$

where q is the number of tied groups and t_p is the number of data values in the p-th group. The standardized test statistic Z follows a standard normal distribution and is computed as follows:

$$Z = \begin{cases} \frac{S-1}{\sqrt{Var(S)}} & if \ S > 0 \\ 0 & if \ S = 0 \\ \frac{S+1}{\sqrt{Var(S)}} & if \ S < 0 \end{cases} \quad (13)$$

At the significance level α, the existing trend is considered to be statistically significant if $p \leq \alpha/2$ in the case of the two-tailed test.

To take account of the presence of autocorrelation in the SPI time series, which might increase the probability to detect trends when actually none exists, the Modified Mann-Kendall test can be applied (Hamed and Rao, 1998). Furthermore, the reason for the use the Modified Mann-Kendal test (MMK) lays in its accuracy for the analysis of correlated data (Hamed and Rao, 1998;Mondal et al., 2012;Sa'adi et al., 2019), which is the case for the SPI time series in this study, compared to the original Mann-Kendall trend test without any loss of power. For this purpose, a modified form of Var(S), set as Var(S)*, is used as follows:

$$Var(S)^* = Var(S)\frac{n}{n^*} \quad (14)$$

where n* is the effective sample size and n the number of observations. The ratio between the effective sample size and the actual number of observations was computed as proposed by (Hamed and Rao, 1998) as follows:

$$\frac{n}{n^*} = 1+\frac{2}{n(n-1)(n-2)}\sum_{i=1}^{n-1}(n-i)(n-i-1)(n-i-2)r_i \quad (15)$$

where: r_i is the lag-i significant auto-correlation coefficient of rank i of time series.

Sen (1968) developed a non-parametric procedure to assess the slope of trend in a sample of N pairs of data:

$$Q_i = \frac{x_j - x_i}{j-i}, i = 1,2,\dots N, j > i \quad \sout{T_i = \frac{x_j - x_i}{j-i},\ i = 1,2,\dots N,\ j > i} \quad (16)$$

where x_j and x_i are data values at time j and i (j>i) respectively. If there is only one datum in each time period, then N =n(n-1)/2, where n is the number of time periods. If there are multiple observations in one or more time periods, then N = n(n-1)/2, where n is the total number of observations.

The N values of Qi are ranked from smallest to largest and the median of slope or Sen's slope estimator is computed as: ~~The Sen's estimator of slope is defined by the median of the N values of T_i:~~

$$Q_{med} = \begin{cases} Q_{\frac{N+1}{2}} & \text{if N is odd} \\ \frac{1}{2}\left[Q_{\frac{N}{2}} + Q_{\frac{N+2}{2}}\right] & \text{if N is even} \end{cases} \quad \sout{T = \begin{cases} Q_{\frac{N+1}{2}} & \text{if N is odd} \\ \frac{1}{2}\left[Q_{\frac{N}{2}} + Q_{\frac{N+2}{2}}\right] & \text{if N is even} \end{cases}} \quad (17)$$

The ~~T~~ Q_{med} sign reflects the data trend behavior (increase or decrease), while its value indicates the steepness of the trend.

2.5 Drought characteristics

To describe meteorological drought features of the studied area, the occurrence of drought events was evaluated for each cell of the gridded dataset according to the SPI threshold and the average over the period of observation was illustrated. Two different thresholds in the SPI value were used, SPI ≤ - 1 and SPI ≤ -2, to detect the behavior of the region with respect to moderate and extremely severe drought conditions (see Table 1). The effect of the accumulation period was investigated. Additionally, three drought characteristics, namely mean drought duration (MDD), mean drought severity (MDS) and mean drought intensity (MDP) (Guo et al., 2018; Wang et al., 2019; Fung et al., 2020) were selected. By linking the SPI data with the "run theory" proposed by (Yevjevich, 1967), and according to (Wang et al., 2019) MDD and MDS were calculated as follows:

$$\text{MDD} = \frac{\sum_{i=1}^{N} \text{DD}_i}{N} \quad (18)$$

$$\text{MDS} = \frac{\sum_{i=1}^{N} \text{DS}_i}{N}, \sout{DS_i\ DS = \sum_{DD_i\ DD} \text{SPI Drought Index Value},\ DS < 0} \quad (14)$$

where, provided a given SPI threshold, DD is the period of time with continuous (negative) values of the SPI below the given threshold (i.e. drought spell duration in the run theory), i is the number of the sequence of DD, N is the total number of drought spells observed during the studied period, DS_i is the value of drought severity associated to the period DD_i (Figure 2). Events

ha formattato: Tipo di carattere: (Predefinito) +Titoli (Times New Roman), Inglese (Regno Unito)

ha formattato: Tipo di carattere: (Predefinito) +Titoli (Times New Roman), Inglese (Regno Unito)

ha formattato: Tipo di carattere: (Predefinito) +Titoli (Times New Roman), Inglese (Regno Unito)

ha formattato: Tipo di carattere: (Predefinito) +Titoli (Times New Roman), Inglese (Regno Unito)

ha formattato: Tipo di carattere: (Predefinito) +Titoli (Times New Roman), Inglese (Regno Unito)

ha formattato: Tipo di carattere: (Predefinito) +Titoli (Times New Roman), Inglese (Regno Unito)

ha formattato: Tipo di carattere: (Predefinito) +Titoli (Times New Roman), Inglese (Regno Unito)

ha formattato: Tipo di carattere: (Predefinito) +Titoli (Times New Roman), 10 pt, Inglese (Regno Unito)

ha formattato: Tipo di carattere: (Predefinito) +Titoli (Times New Roman), Inglese (Regno Unito)

ha formattato: Tipo di carattere: (Predefinito) +Titoli (Times New Roman), Inglese (Regno Unito)

ha formattato: Inglese (Regno Unito)

ha formattato: Pedice

with DD ≥ 3 months were only accounted for. Additionally, the mean drought intensity MDP was computed as the ratio between MDS and MDD (Li et al., 2017). As in the case of the computation of MDD, MDS and MDP, the two different thresholds, SPI ≤ - 1 and SPI ≤ -2, were taken into consideration. The effect of the accumulation scale and the spatial patterns were investigated.

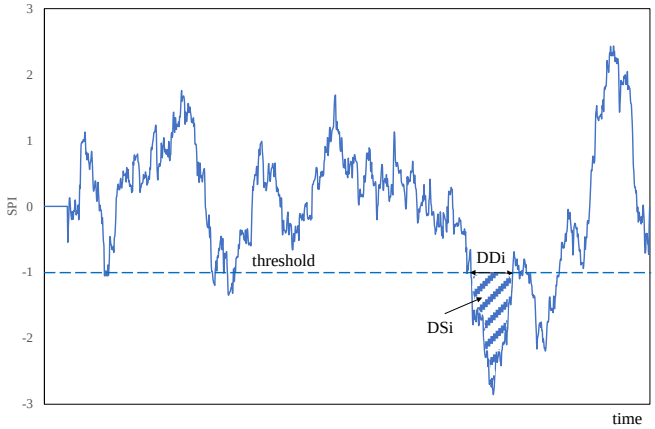

Figure 2. Drought characteristics identification using the 'run theory' (Yevjevich, 1967).

3. Results and discussion

3.1 Temporal analysis

The temporal patterns of the SPI time series in the region under investigation at different time scales have the potential to provide insights into the temporal variation of droughts in the Campania. As an example, Figure 3 illustrates SPI_6, SPI_12 and SPI_24 for two cells of the grid data (Figure 1). In the left panel an example from the southern coastal area is depicted whereas in the right panel an example from the northern inland area.

In both areas, Figure 3 clearly highlights the drought periods that affected the Campania region around the 1940-1950 and around 1990-2010. This result appears coherent with a European scale assessment study where it was reported that the period between 1985-1995 was characterized by the broadest spread of extreme drought events, mainly localized on the Iberian Peninsula, Southern Europe, the Balkans and Western Turkey (Bonaccorso et al., 2013). Drought severity appears less pronounced in the northern inland areas, especially if looking at the longest accumulation time scale. Drought tends to be more persistent in the southern areas rather than in northern one which additionally have been only a little impacted by the drought conditions started in the 2015 in the region. More details about the spatial variability of drought features will be discussed in the following.

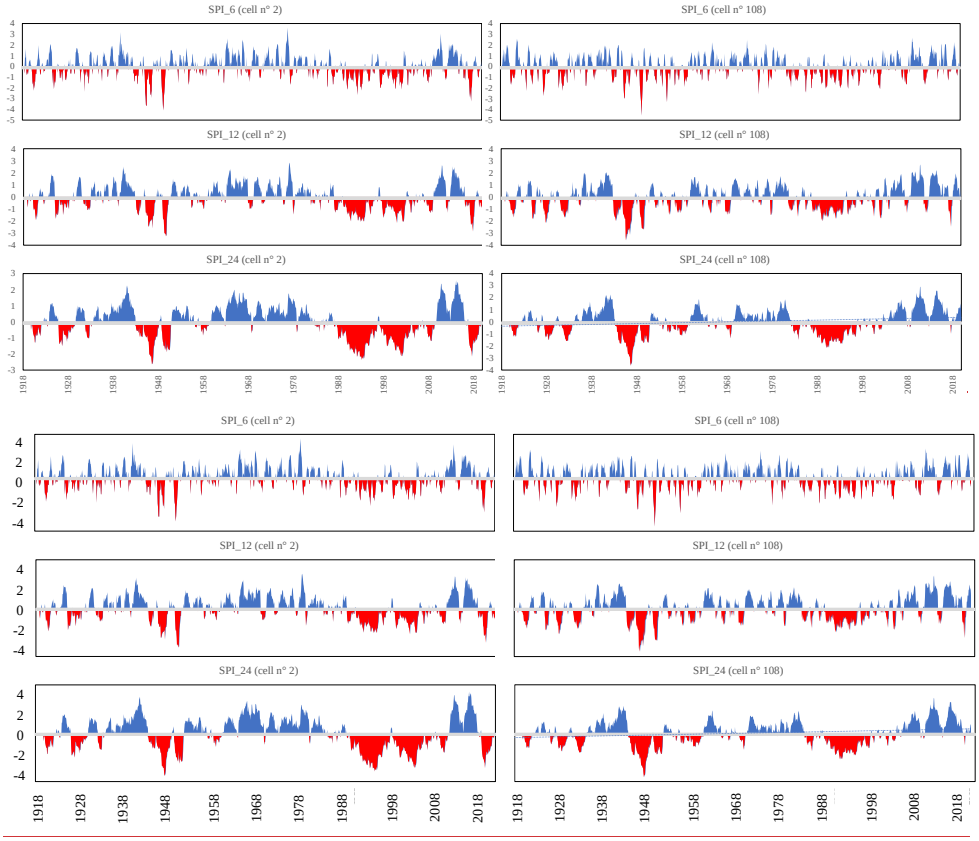

Figure 3. SPI_6, SPI_12 and SPI_24 for cell n°2 (southern area – left panel) and cell n° 108 (northern area – right area).

The Modified Mann-Kendall (MMK) test and the Sen's slope estimator were carried out to investigate temporal trends, sign, significance and magnitude in SPI time series over the studied period. The relevant results of the Modified Mann-Kendall (MMK) for trend sign and significance (significance level = 5%) are shown respectively in Figure 4 and Figure 5.

Starting from the SPI_3 to SPI_12, the downward trend become dominant in the study area and especially marked in the northwest and south sectors of the region (Figure 4), which correspond to the area featured by the largest mean annual precipitation and the largest precipitation downward trend (Longobardi and Villani, 2010). The proportion of negative to positive trend, with negative values still dominant in over 60% of the cells, remains almost similar for the SPI_24 to SPI_48.

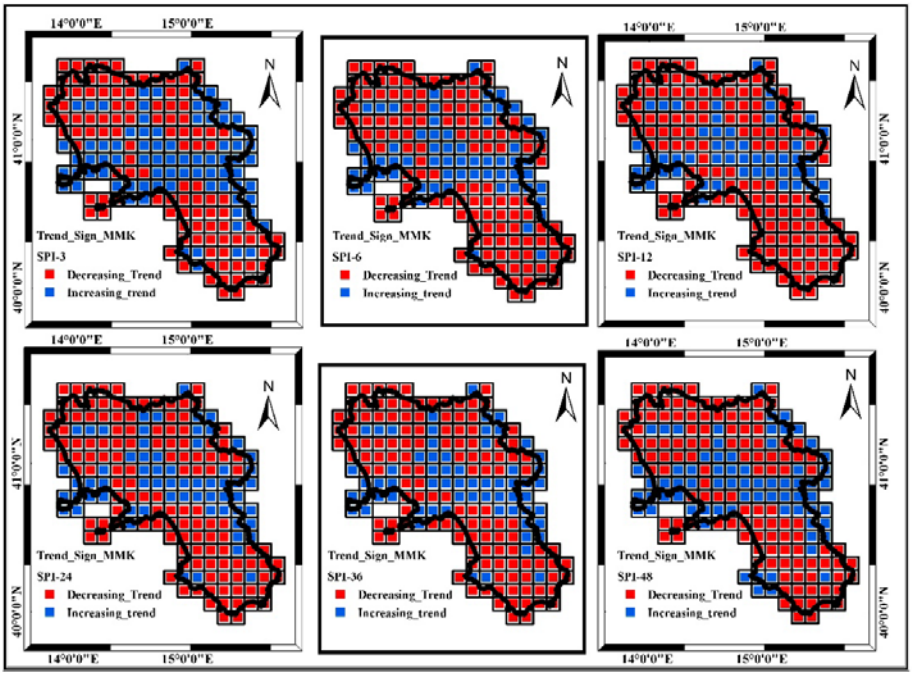

Figure 4: SPI MMK test sign, for the different accumulation scales (α = 5 %). ~~Trasforma le frecce in colori (se vuoi anche come la figura seguente) perché continua ad essere difficile la visione distinta.~~

For what concern the significance of the trend (Figure 5), the MMK test illustrated how a very large proportion of the gridded SPI showed a significant trend over the different time scales especially from the SPI_3 to the SPI_24 accumulation scale (Figure 5). For the SPI_3, SPI_6 and SPI_12, the negative trend is particularly significant, with a percentage of grid cells of about 55 % for both SPI_3 and SPI_6 and 65% for SPI_12. Regarding the spatial distribution of the trend, the SPI_24 is the most significant with almost 70% of the grid cells. Beyond this scale, temporal variations did not appear significant. As ~~, and this could represent an indication that likely the~~ the groundwater systems of the region are~~, frequently~~ characterized by ~~very~~ large delay times thus potentially impacted by SPI accumulated over large scale, it is likely that those systems are not strongly ~~could not be~~ impacted by climate temporal variations (Longobardi and Van Loon, 2018). On the national scale the obtained

results were well in line with the general overview outlined in a previous research by Delitala et al. (2000) and Bordi et al. (2001) for other regions of southern Italy (Sardinia, Sicily and Puglia) and, furthermore, were in perfect accord with the outcomes given by Buttafuoco and Caloiero (2014) for the Calabria region in southern Italy.

At the regional scale, the results for the modified Mann-Kendall trend test, ~~were~~ are also coherent with the findings of previous climatological studies concerning precipitation regime investigation (Longobardi and Villani, 2010; Longobardi et al., 2016). In fact, annual and seasonal precipitation in the region were found to be featured by a generalized negative trend during the last century, even though the downward tendencies, contrary to the SPI tendencies, were significant for a very moderate number of rain gauge stations.

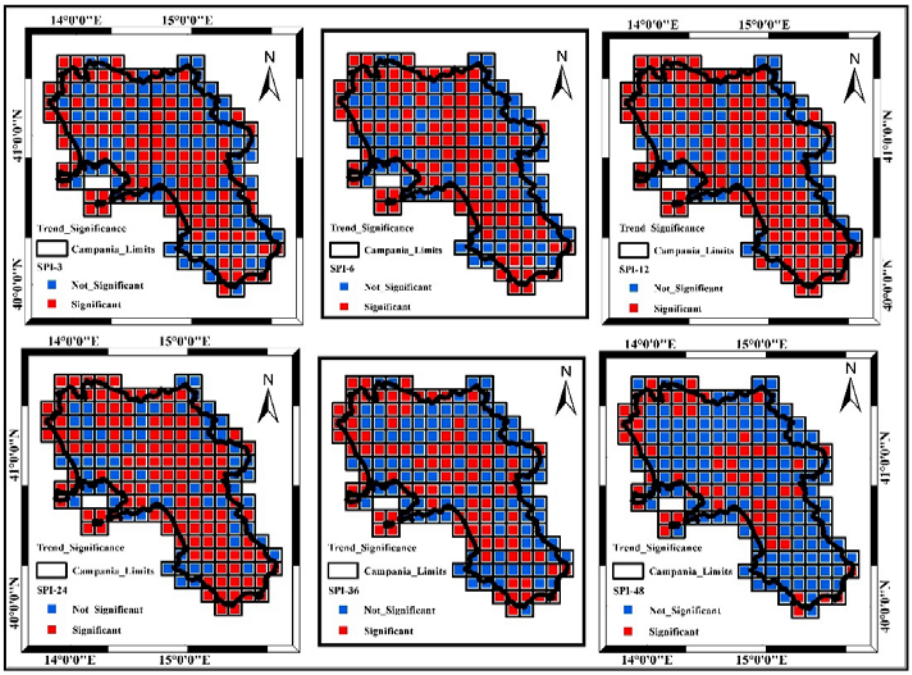

Figure 5: SPI MMK test significance (α = 5 %), for the different accumulation scales.

The magnitude of the trend in the SPI time series, as assessed using Sen's estimator, is presented in Figure 6. In agreement with the results of the MMK test, the trend was dominantly negative across the region, coherently with the trend sign represented in Figure 4, with some exception for a west-east transect at the middle latitude of the region, which corresponds

to an area which is featured by moderate mean annual precipitation values and the lowest downward precipitation trends (Longobardi and Villani, 2010). On average, the tendency toward drier conditions was however rather moderate and characterized by an amplification with increasing accumulation time scale. The increase in the SPI index amount to about 10%, in ten years for the case of SPI_6. It increases up to 15% ~~to~~ and 24%, in ten years, respectively for the case of SPI_12 and SPI_48. The variability in the minimum and maximum assessed trend, on the spatial scale, also increases for increasing accumulation time scale.

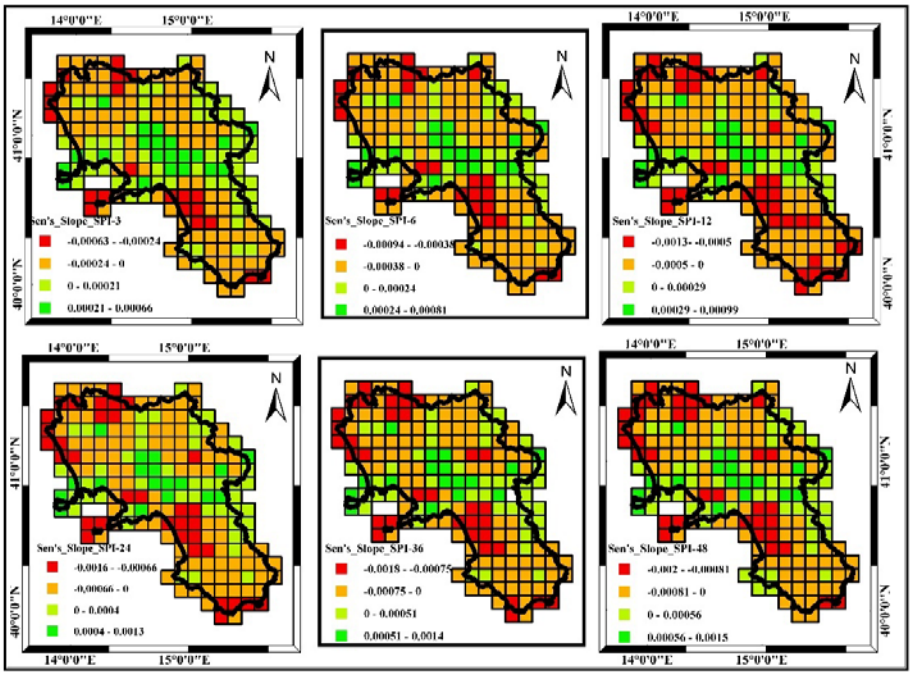

Figure 6: SPI Sen's slope, for the different accumulation time scales.

3.2 Drought characteristics assessment

Figure 7 shows the total number of drought events detected within the SPI time series from 1918 to 2019 for moderate drought conditions (threshold SPI ≤ - 1) and for extremely severe drought conditions (threshold SPI ≤ - 2) for each point of the grid for all the accumulation scales considered. In the case of moderate drought events, it was observed that the SPI_3 is associated

to the largest number of droughts, which was on average 95, for the whole period of observation, over the 191 grid cells. Provided the large theoretical autocorrelation in SPI timeseries for the larger accumulation scale, drought frequency decreased with increasing accumulation scale, with the SPI_24 to SPI_48 patterns almost similar among them (Figure 7 upper panel). The results appeared in good agreement with what demonstrated by other authors (McKee et al., 1993; Buttafuoco et al., 2015; Marini et al., 2019; Fung et al., 2020). A very similar behavior was found in the case of extremely severe droughts episodes, unless for the lower number compared to the case of moderate events. The average number of drought events in the case of SPI_3 for the threshold SPI ≤ - 2, was on average 27, for the whole period of observation, over the 191 grid cells. For what concerns the spatial patterns, although a moderate correlation appeared for small cluster of cells, it was not found an evident concentration of drought events occurrence in a specific area.

SPI = -1

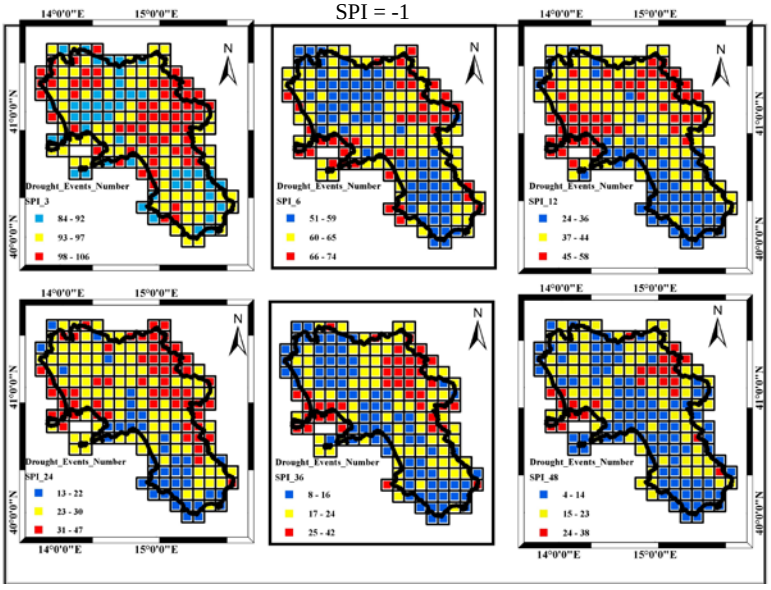
14°0'0"E
15°0'0"E
N
Drought_Events_Number
SPI_3
84 - 92
93 - 97
98 - 106
SPI_6
51 - 59
60 - 65
66 - 74
SPI_12
24 - 36
37 - 44
45 - 58
SPI_24
13 - 22
23 - 30
31 - 47
SPI_36
8 - 16
17 - 24
25 - 42
SPI_48
4 - 14
15 - 23
24 - 38

SPI = -2

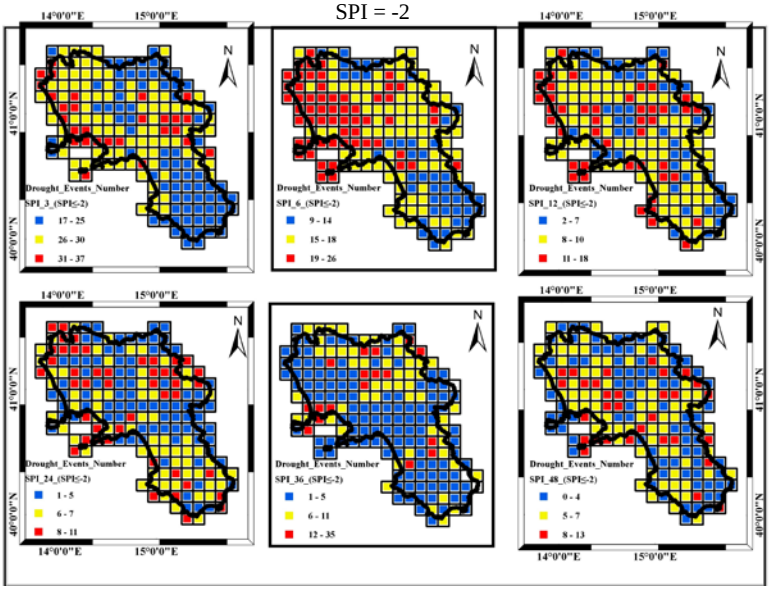
14°0'0"E
15°0'0"E
N
Drought_Events_Number
SPI_3_(SPI≤-2)
17 - 25
26 - 30
31 - 37
SPI_6_(SPI≤-2)
9 - 14
15 - 18
19 - 26
SPI_12_(SPI≤-2)
2 - 7
8 - 10
11 - 18
SPI_24_(SPI≤-2)
1 - 5
6 - 7
8 - 11
SPI_36_(SPI≤-2)
1 - 5
6 - 11
12 - 35
SPI_48_(SPI≤-2)
0 - 4
5 - 7
8 - 13

Figure 7: Drought event numbers, for the different accumulation time scales, over the whole period of observation 1918-2019. Upper panel: moderate drought events (SPI ≤ - 1). Lower panel: extremely severe drought events (SPI ≤ - 2)

More insights came from the analysis of the MDD, MDS and MDP, respectively illustrated in Figure 8, 9 and 10 with reference to a threshold value of SPI ≤ -1.

For what concerns the MDD (Figure 8), differently from what occurred in terms of drought frequency, the mean drought duration increased with the accumulation time scale, ranging from 4 to 5 months for the SPI_3, to 8 to 60 months for the SPI_48. The accumulation time scale also affected the MDD spatial behaviour (Figure 8). In the case of SPI_3 and SPI_6, almost the whole region was affected by the average MDD values. In the case of SPI_12, SPI_24, SPI_36 and SPI_48, the largest MDD values were detected along a north-west to south-east transect and however more evidently in the southern sectors of the region. At the smallest time scales (SPI_3) the northern sections are the most impacted. For the larger accumulation time scales, the maximum values detected in the southern region were mainly caused by severe drought periods occurred in the '90, 2003 and 2017 in the region.

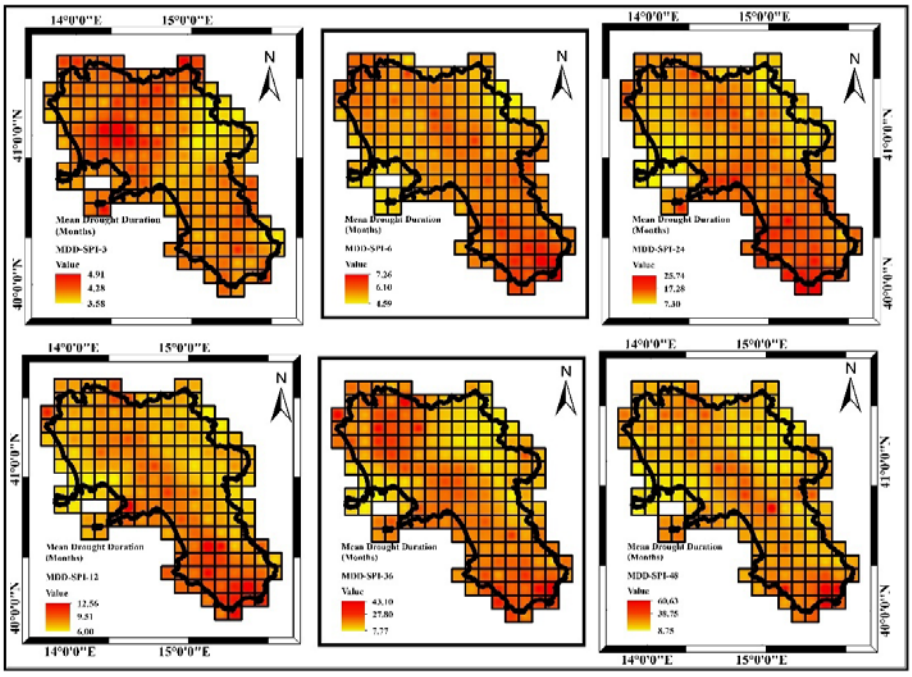

Figure 8: MDD (mean drought duration) for the different considered accumulation periods (SPI ≤ -1).

For what concerned the MDS (Figure 9), because of the MDD characteristics, the drought severity increased with the accumulation time scale ranging from 6 to 8 for the SPI_3, to 11 to 90 for the SPI_48 (Figure 9). The spatial pattern of MDS was affected by the accumulation time scale, such as in the case of the MDD. For the SPI_3, MDS showed a major severity in the northern area, whereas moving from SPI_12 to SPI_48, MDS severity moved from northern to southern areas and almost disappeared with an evenly distribution set on an almost constant value (about -10).

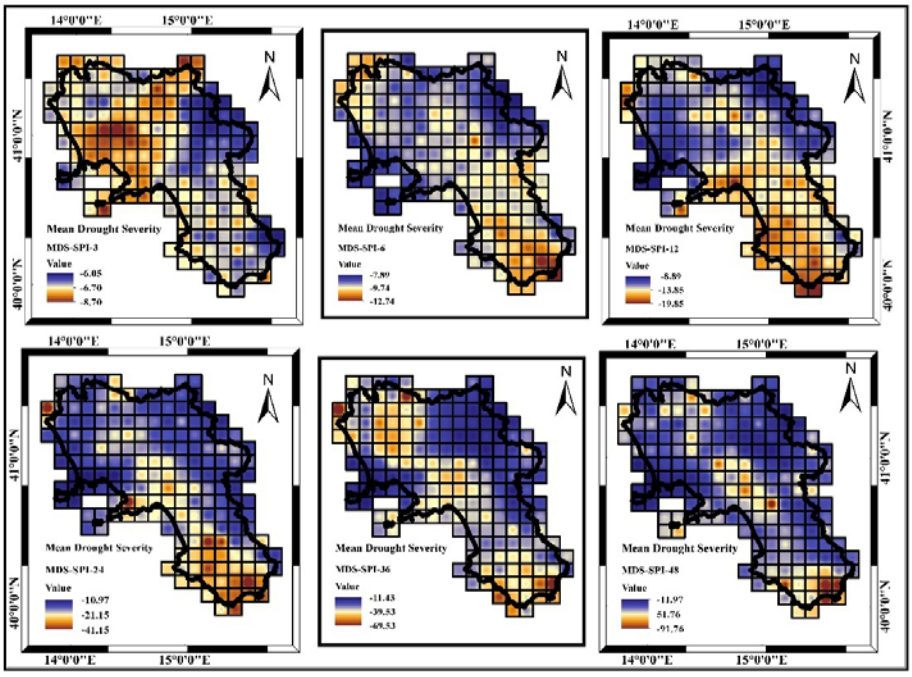

Figure 9: MDS (mean drought severity) for the different considered accumulation periods (SPI ≤ -1).

For what concerned the MDP (Figure 10), because of what previously observed in the case of the MDD and MDS, the minimum (about -1.5 on average) and maximum (about -2.3 on average) values appeared similar for the different accumulation time scale, likely more pronounced for the lower accumulation scales, where MDP largest peaks are focused on the northern area. Differently, the spatial pattern was found to be particularly complex and did not show a clear tendency related to the accumulation time scale (Figure 10). Overall, the largest peaks are detected in the northern areas of the region for the SPI_3 to SPI_6. From SPI_24 to SPI_48 there was a general tendency for a dominant low peak spatial distribution, with an exception for some coastline areas in the north of the region. The SPI_12 represented a neutral condition, where minimum and maximum SPI values are rather pronounced and spread over the region.

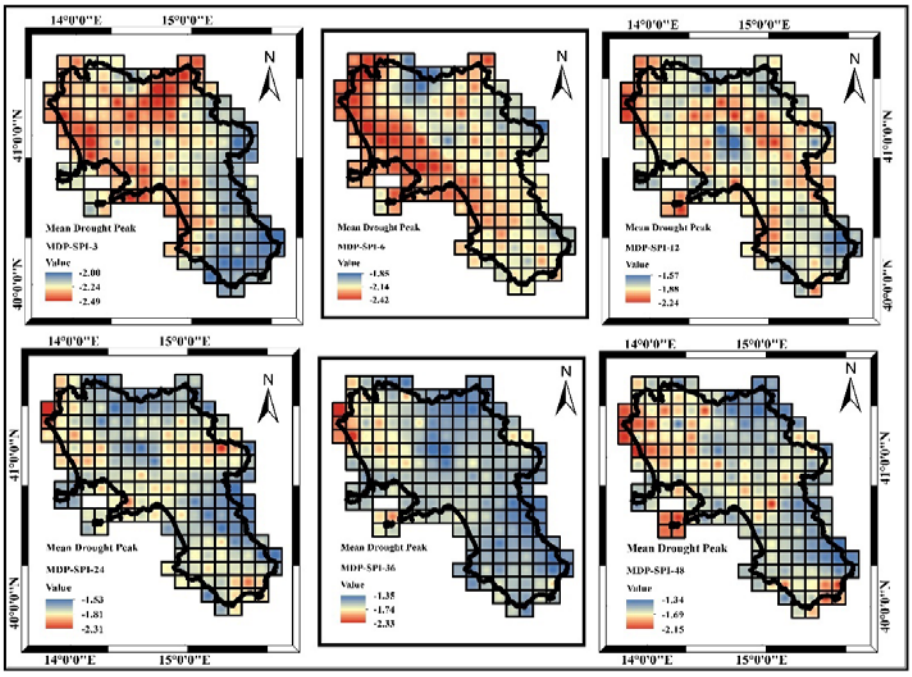

Figure 10: MDP (mean drought peak) for the different considered accumulation periods (SPI ≤ -1).

By increasing the threshold for the SPI values, moving from SPI ≤ - 1 to SPI ≤ - 2, it was possible to explore the extremely severe drought conditions over the region.

For wat concerned the MDD (Figure 11), the mean drought duration increased with the accumulation time scale, ranging from 3 months for the SPI_3, to 47 months for the SPI_48. Compared to the case of moderate drought events, in the case of extremely severe events the mean drought duration decreased for each accumulation scale. For what concerned the spatial distribution, the same consideration provided for the case of SPI threshold ≤ -1 hold also in the case of SPI threshold ≤ -2.

With reference to the MDS, accordingly to the MDD, the drought severity increased with the accumulation time scale ranging from 16 for the SPI_3, to 109 for the SPI_48 (Figure 12). Compared to the case of moderate drought events, in the case of extremely severe events the mean drought severity increased for each accumulation scale. For what concerned the spatial pattern of MDS, it appeared a common feature according to which the largest MDS values appeared in the central area of the

region, with some spot cells located in the extremely southern and extremely northern coastline. An exception was provided by the lower SPI_3.

In the end, for what concerned the MDP (Figure 13), differently to what occurred in the case of the MDD and MDS, the minimum (about -2.5 on average) and maximum (about -3.5 on average) values appeared similar for the different accumulation time scale, likely more pronounced for the lower accumulation scales (-4.09 for SPI_6). The spatial pattern was found to be particularly complex and did not show a clear tendency related to the accumulation time scale (Figure 13). Larger peaks were still focused in the central area of the region, but the area covered changed with accumulation time scale, being rather moderate for the larger SPI accumulation scale. Large peak appeared to spread all over the region in the case of the largest accumulation periods, for SPI_36 and SPI_48.

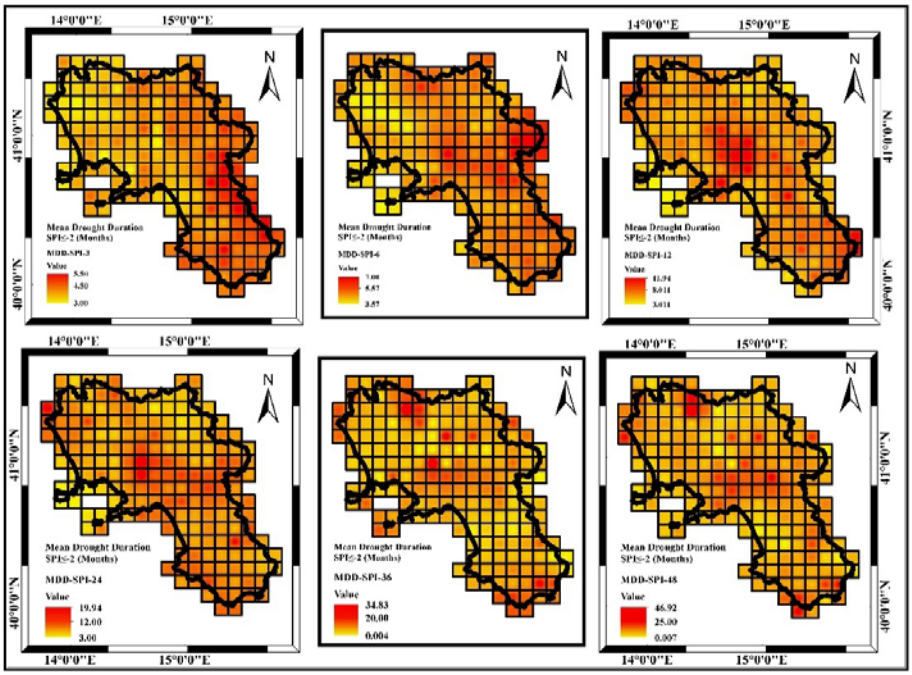

Figure 11: MDD (mean drought duration) for the different considered accumulation periods (SPI ≤ -2).

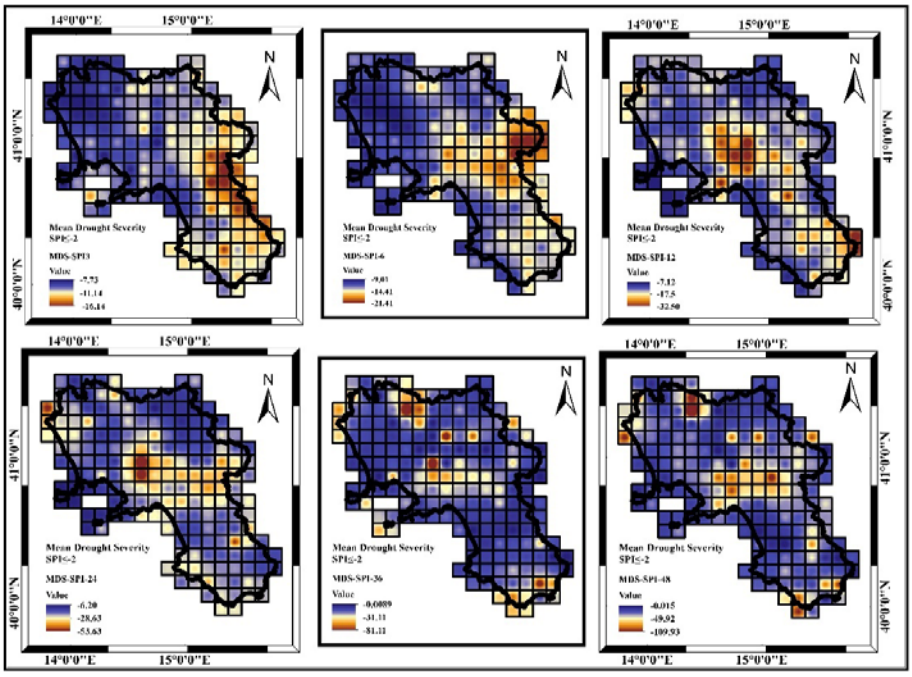

Figure 12: MDS (mean drought severity) for the different considered accumulation periods (SPI ≤ -2).

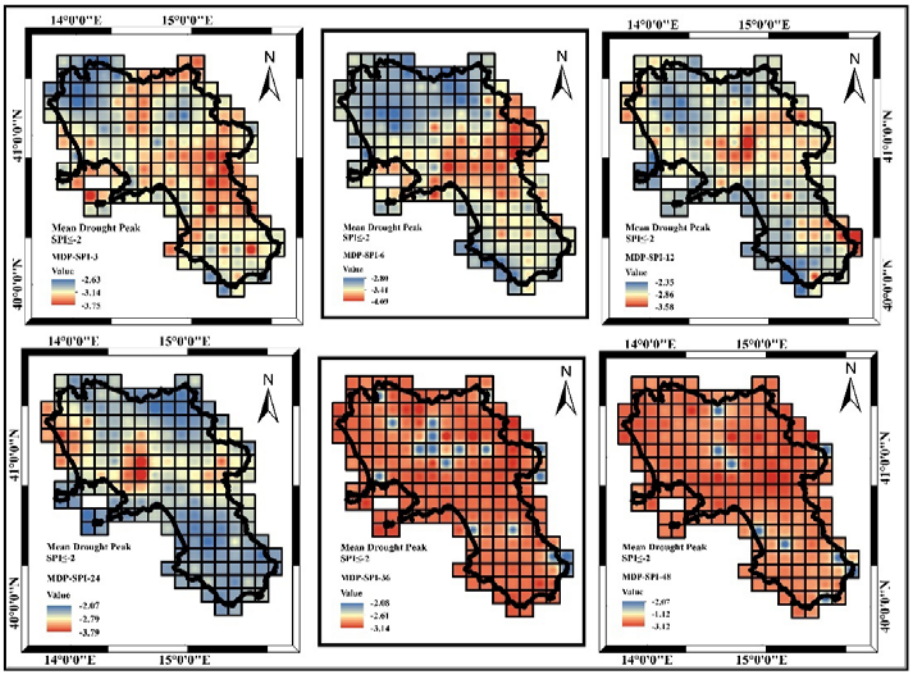

Figure 13: MDP (mean drought peak) for the different considered accumulation periods (SPI ≤ -2).

4. Conclusions

Drought is a sustained period of below-normal water availability. It is a recurring and worldwide phenomenon, but the Mediterranean basin is seen as a very vulnerable environment in this perspective. The main objective of this study was to assess the drought features in the Campania region of southern Italy through an analysis of the spatial and temporal patterns characteristics of SPI time series, computed at different accumulation scales, over a centennial period, from 1918 to 2019. The Modified Mann-Kendall test and the Sen's test were applied to describe the temporal trend significance and magnitude. Additionally, for both moderate (SPI ≤ -1) and extremely severe (SPI ≤ -2) drought conditions, the "run theory" (Yevjevich, 1967) was applied to illustrate drought events frequency, duration, peak and severity.

For what concerns the drought temporal features, the trend was found to be dominantly negative and the percentage of impacted cells increased with accumulation scale. It remained almost similar for SPI time series computed over 24 months or larger

intervals. The significance was also found to be particularly evident approaching 70% of grid cells for SPI_24. Beyond this time scale threshold, significance in temporal variability strongly decreased. The SPI increase over time ranged from about 10%, in ten years, for the case of SPI_6 ~~to~~ and 24%~~, in ten years, for the case of~~ for the SPI_48. In the case of moderate dry conditions, MDD increased with the accumulation time scale, ranging from about 5 months for the SPI_6, to 60 months for the SPI_48. Accordingly, MDS increased with accumulation scale, moving from about -10 in the case of SPI_6 to about -50 in the case of SPI_48. MDP did not changed significantly with the accumulation scale and was particularly pronounced in the case of the lower temporal scales. Extremely severe events were featured by lower durations and larger severity compared to the moderate drought events but were very less frequent (over 75% less then).

For what concerned the spatial pattern, the negative trends appeared to occur along a north-west to south-east transect, whereas positive trend were focused along a west-east transect at the middle latitude of the region. These areas are respectively featured by large mean annual precipitation coupled with the largest negative trends and by low to moderate mean annual precipitation and lowest negative trends. Those two regions are quite different in terms of orography. While the first is characterized by relieves approaching or close to the coastline, the second is featured by a large plain devoted to agricultural practic~~i~~es, crossed by the longest river of the region, the Volturno River, which probably represents an access corridor to atmospheric weather systems. The complex orography of the region appears then to impact both the average precipitation spatial distribution as well as the relevant temporal variability. The accumulation time scale affected the MDD spatial behavior. At the lowest accumulation scale, the northern area appeared to be more affected whereas large MDD values were detected along a north-west to south-east transect and however more evidently in the southern sectors of the region. The maximum values detected in the southern area for the larger accumulation time scale were mainly caused by severe drought periods occurred in the '90, 2003 and 2017 in the region. MDS spatial pattern was also affected by accumulation scale. It showed a ~~focus~~ concentration on the northern region area for the lower temporal scales and instead a constant spatial distribution for the larger temporal scales, with an exception for a north-west to south-east transect and however for the southern sectors of the region where the largest MDS values were detected. In the end, the MDP spatial pattern was found to be particularly complex and did not show a clear tendency related to the accumulation time scale. At least, for the smaller time scale, the largest drought peaks seemed ~~focused~~ concetrated on the norther inland area of the region, which overall could be addressed as an area potentially prone to agricultural droughts stress.

The reported research illustrated how historical in-situ long term measurements are crucial for understanding historical drought conditions to plan mitigation strategies to further face future climate change impacts.

Author contribution: AL and PV contributed to the conceptualization. AL and OB contributed to data curation and formal analysis. AL and PV provided supervision and AL and OB the writing of the original draft. Al, OB and PV contributed to the revised manuscript version.

Competing interests: The authors declare that they have no conflict of interest.

Acknowledgments

Authors would like to tank anonymous referees for their encouragements and helpful comments which resulted in an improved manuscript version. Furthermore, authors would like to thanks Valentina Nobile and Marco Sessa for their effective support in data collection.

References

Abramowitz, M., and Stegun, I. A.: Handbook of mathematical functions with formulas, graphs, and mathematical tables, US Government printing office, 1964.

Bonaccorso, B., Peres, D.J., Cancelliere, A., Rossi, G. Large Scale Probabilistic Drought Characterization Over Europe (2013) Water Resources Management, 27 (6), pp. 1675-1692.

Bonaccorso, B., Aronica, G.T.: Estimating Temporal Changes in Extreme Rainfall in Sicily Region (Italy), Water Resour Manag, 30 (15), 5651-5670, 2016.

Bordi, I., Frigio, S., Parenti, P., Speranza, A., and Sutera,: The analysis of the Standardized Precipitation Index in the Mediterranean area: regional patterns, ANN GEOPHYS-ITALY., 44, 2001.

Boulariah, O., Longobardi, A., Nobile, V., Sessa, M. and Villani, P.: Long term monthly precipitation database reconstruction for drought assessment. In: "ClimRisk2020: Time for Action! Raising the ambition of climate action in the age of global emergencies" – SISC Seventh Annual Conference, 21-23 October 2020, 2020.

Buttafuoco, G., and Caloiero,: Drought events at different timescales in southern Italy (Calabria), J MAPS., 10, 529-537, 2014.

Buttafuoco, G., Caloiero, T., and Coscarelli, R.: Analyses of drought events in Calabria (southern Italy) using standardized precipitation index, WATER RESOUR MANAG., 29, 557-573, 2015.

Caloiero, T., Veltri, S., Caloiero, P., and Frustaci, F.: Drought analysis in Europe and in the Mediterranean basin using the standardized precipitation index, Water., 10, 1043, 2018.

Caloiero, T., Veltri, S., A.: Drought assessment in the Sardinia Region (Italy) during 1922–2011 using the standardized precipitation index, J APPL GEOPHYS., 176, 925-935, 2019.

Capra, A., Scicolone, B., a: Spatiotemporal variability of drought on a short–medium time scale in the Calabria Region (Southern Italy), Theor. Appl. Climatol., 110, 471-488, 2012.

Cook, B. I., Anchukaitis, K. J., Touchan, R., Meko, D. M., and Cook, E. R.: Spatiotemporal drought variability in the Mediterranean over the last 900 years, J. Geophys. Res. Atmos., 121, 2060-2074, 2016.

Delitala, A. M., Cesari, D., Chessa, P. A., and Ward, M. N.: Precipitation over Sardinia (Italy) during the 1946–1993 rainy seasons and associated large-scale climate variations, INT J CLIMATOL., 20, 519-541, 2000.

Di Lena, B., Vergni, L., Antenucci, F., Todisco, F., Mannocchi, F.: Analysis of drought in the region of Abruzzo (Central Italy) by the Standardized Precipitation Index, Theor. Appl. Climatol 115, 41-52, 2014.

Dracup, J. A., Lee, K. S., and Paulson Jr, E. G.: On the definition of droughts, Water Resour. Res.,16, 297-302, 1980.

European drought center., http://europeandroughtcentre.com/, last access: 10 December 2020.

Fung, K., Huang, Y., and Koo, C.: Assessing drought conditions through temporal pattern, spatial characteristic and operational accuracy indicated by SPI and SPEI: case analysis for Peninsular Malaysia, NAT HAZARDS., 103, 2071-2101, 2020.

Gaitán, E., Monjo, R., Pórtoles, J., Pino-Otín, M.R. Impact of climate change on drought in Aragon (NE Spain) (2020) Science of the Total Environment, 740, art. no. 140094 .

Ganguli, P., and Reddy, M. J.: Evaluation of trends and multivariate frequency analysis of droughts in three meteorological subdivisions of western India, INT J CLIMATOL., 34, 911-928, 2014.

Gouveia, C., Trigo, R. M., Beguería, S., Vicente-Serrano, S. M.: Drought impacts on vegetation activity in the Mediterranean region: An assessment using remote sensing data and multi-scale drought indicators, GLOBAL PLANET CHANGE .,151, 15-27, 2017.

Guo, H., Bao, A., Liu, T., Ndayisaba, F., Jiang, L., Kurban, A., and De Maeyer, P.: Spatial and temporal characteristics of droughts in Central Asia during 1966–2015, SCI TOTAL ENVIRON.,624, 1523-1538, 2018.

Hamed, K. H., and Rao, A. R..: A modified Mann-Kendall trend test for autocorrelated data, J HYDROL .,204, 182-196, 1998.

Hasegawa, A., Gusyev, M., and Iwami, Y.: Meteorological drought and flood assessment using the comparative SPI approach in Asia under climate change, J. Disaster Res. .,11, 1082-1090, 2016.

Husak, G. J., Michaelsen, J., and Funk, C.: Use of the gamma distribution to represent monthly rainfall in Africa for drought monitoring applications, INT J CLIMATOL.,27, 935-944, 2007.

IPCC, 2014: Climate Change 2014: Synthesis Report. Contribution of Working Groups I, II and III to the Fifth Assessment Report of the Intergovernmental Panel on Climate Change [Core Writing Team, R.K. Pachauri and L.A. Meyer (eds.)]. IPCC, Geneva, Switzerland, 151 pp.

Kendall, M. G.: Rank correlation methods, 1948.

LI, X.-X., JU, H., Sarah, G., YAN, C.-R., Batchelor, W.D., LIU, Q.: Spatiotemporal variation of drought characteristics in the Huang-Huai-Hai Plain, China under the climate change scenario, J. Integr. Agr., 16 (10), 2308-2322, 2017.

Littell, J. S., Peterson, D. L., Riley, K. L., Liu, Y., and Luce, C. H.: A review of the relationships between drought and forest fire in the United States, GLOB CHANGE BIOL., 22, 2353-2369, 2016.

Liu, Z., Wang, Y., Shao, M., Jia, X., and Li, X.: Spatiotemporal analysis of multiscalar drought characteristics across the Loess Plateau of China, J HYDROL.,534, 281-299, 2016.

Longobardi, A., and Villani, P.: Trend analysis of annual and seasonal rainfall time series in the Mediterranean area, INT J CLIMATOL., 30, 1538-1546, 2010.

Longobardi, A., and Mautone, M.: Trend analysis of annual and seasonal air temperature time series in southern Italy, in: Engineering Geology for Society and Territory-Volume 3, Springer, 501-504, 2015.

Longobardi, A., Buttafuoco, G., Caloiero, T., Coscarelli, R.: Spatial and temporal distribution of precipitation in a Mediterranean area (southern Italy), Environ. Earth Sci., 75 (3), art. no. 189, 1-20, 2016.

Longobardi, A., and Van Loon, A. F.: Assessing baseflow index vulnerability to variation in dry spell length for a range of catchment and climate properties, HYDROL PROCESS., 32, 2496-2509, 2018.

Longobardi, A., and Boulariah, O.: Long term regional changes in inter-annual precipitation variability in a Mediterranean area, THEOR APPL CLIMATOL, under review.

Mann, H. B.: Nonparametric tests against trend, Econometrica., 245-259, 1945.

Marini, G., Fontana, N., Mishra, A. K.: Investigating drought in Apulia region, Italy using SPI and RDI, Theor. Appl. Climatol .,137, 383-397, 2019.

Martinez, C., Goddard, L., Kushnir, Y., and Ting, M.: Seasonal climatology and dynamical mechanisms of rainfall in the Caribbean, Clim.Dynam.,53, 825-846, 2019.

McKee, T. B., Doesken, N. J., and Kleist, J.: The relationship of drought frequency and duration to time scales,in: Proceedings of the 8th Conference on Applied Climatology, 179-183, 1993

Mishra, A. K., and Singh, V. P.: A review of drought concepts, J HYDROL., 391, 202-216, 2010.

Mondal, A., Kundu, S., Mukhopadhyay, A.: Rainfall trend analysis by Mann-Kendall test: A case study of north-eastern part of Cuttack district, Orissa, Int. J. Geol. Earth Sci 2, 70-78, 2012.

Pachauri, R. K., Allen, M. R., Barros, V. R., Broome, J., Cramer, W., Christ, R., Church, J. A., Clarke, L., Dahe, Q., and Dasgupta, P.: Climate change 2014: synthesis report. Contribution of Working Groups I, II and III to the fifth assessment report of the Intergovernmental Panel on Climate Change, Ipcc, 2014.

Palmer, W. C.: Meteorological drought, US Department of Commerce, Weather Bureau, 1965.

Palmer, W. C.: Keeping track of crop moisture conditions, nationwide: the new crop moisture index, 1968.

Peres, D.J., Senatore, A., Nanni, P., Cancelliere, A., Mendicino, G., Bonaccorso, B. Evaluation of EURO-CORDEX (Coordinated Regional Climate Downscaling Experiment for the Euro-Mediterranean area) historical simulations by high-quality observational datasets in southern Italy: Insights on drought assessment (2020) Natural Hazards and Earth System Sciences, 20 (11), pp. 3057-3082.

Rouse, J., Haas, R. H., Schell, J. A., and Deering, D. W.: Monitoring vegetation systems in the Great Plains with ERTS, NASA Spec. Publ. 351, 309, 1974.

Ruffault, J., Martin-StPaul, N., Pimont, F., Dupuy, J.-L.: How well do meteorological drought indices predict live fuel moisture content (LFMC)? An assessment for wildfire research and operations in Mediterranean ecosystems, Agric For Meteorol .,262, 391-401, 2018.

Sa'adi, Z., Shahid, S., Ismail, T., Chung, E.-S., Wang, X.-J.: Trends analysis of rainfall and rainfall extremes in Sarawak, Malaysia using modified Mann–Kendall test, METEOROL ATMOS PHYS.;131, 263-277, 2019.

Sobral, B. S., de Oliveira-Júnior, J. F., de Gois, G., Pereira-Júnior, E. R., de Bodas Terassi, P. M., Muniz-Júnior, J. G. R., Lyra, G. B., and Zeri, M.: Drought characterization for the state of Rio de Janeiro based on the annual SPI index: trends, statistical tests and its relation with ENSO, Atmos Res., 220, 141-154, 2019.

Spinoni, J., Naumann, G., Vogt, J. V., and Barbosa, P.: The biggest drought events in Europe from 1950 to 2012, J. Hydrol. Reg. Stud., 3, 509-524, 2015.

Spinoni, J., Barbosa, P., De Jager, A., McCormick, N., Naumann, G., Vogt, J. V., Magni, D., Masante, D., and Mazzeschi, M.: A new global database of meteorological drought events from 1951 to 2016, J. Hydrol. Reg. Stud., 22, 100593, 2019.

Stagge, J. H., Kohn, I., Tallaksen, L. M., and Stahl, K.: Modeling drought impact occurrence based on meteorological drought indices in Europe, J HYDROL., 530, 37-50, 2015.

Stagge, J. H., Kingston, D. G., Tallaksen, L. M., and Hannah, D. M.: Observed drought indices show increasing divergence across Europe, SCI REP-UK ., 7, 1-10, 2017.

Swain, S., and Hayhoe, K.: CMIP5 projected changes in spring and summer drought and wet conditions over North America, Clim.Dynam., 44, 2737-2750, 2015.

Tsakiris, G., and Vangelis, H.: Establishing a drought index incorporating evapotranspiration, European.water.,9, 3-11, 2005.

Van Loon, A. F.: Hydrological drought explained, Wiley Interdiscip. Rev. Water ., 2, 359-392, 2015.

Vicente-Serrano, S. M., Beguería, S., and López-Moreno, J.: A multiscalar drought index sensitive to global warming: the standardized precipitation evapotranspiration index, J CLIMATE ., 23, 1696-1718, 2010.

Wang, J., Lin, H., Huang, J., Jiang, C., Xie, Y., and Zhou, M.: Variations of drought tendency, frequency, and characteristics and their responses to climate change under CMIP5 RCP scenarios in Huai river basin, China, Water., 11, 2174, 2019.

Wilhite, D. A., and Glantz, M. H.: Understanding: the drought phenomenon: the role of definitions, WATER INT ., 10, 111-120, 1985.

Yevjevich, V. M.: Objective approach to definitions and investigations of continental hydrologic droughts, An, Colorado State University. Libraries, 1967.

Yves, T., Koutroulis, A., Samaniego, L., Vicente-Serrano, S. M., Volaire, F., Boone, A., Le Page, M., Llasat, M. C., Albergel, C., and Burak, S.: Challenges for drought assessment in the Mediterranean region under future climate scenarios, EARTH-SCI REV., 103348, 2020.

Zhang, L., and Zhou, T.: Drought over East Asia: a review, J CLIMATE., 28, 3375-3399, 2015.

Zhou, H., and Liu, Y.: SPI based meteorological drought assessment over a humid basin: Effects of processing schemes, Water., 8, 373, 2016.